IOP Astronomy

Modeling and Analysis of Eclipsing Binary Stars
The theory and design principles of PHOEBE
Andrej Prša

Chapter 4

Radiation: The Basics

The computation of fluxes from an extended object has quite a few twists and turns that can trip even a seasoned researcher, so we provide here a step-by-step discussion for the Sun–Earth system in two atmosphere approximations: blackbody and Castelli & Kurucz (2004) model atmosphere. Before we dive into the examples themselves, we need to define several radiative quantities that frame the problem we are trying to solve.

4.1 Intensity

When we measure "light" from a resolved source, we typically measure the amount of energy dE_λ per unit time dt per unit wavelength $d\lambda$ in a beam $d\Omega$ that is radiated from the direction-projected unit area $dA\cos\theta$ (see Figure 4.1):

$$I_\lambda = \frac{dE_\lambda}{dt\ dA\cos\theta\ d\lambda\ d\Omega}. \tag{4.1}$$

This equation defines *intensity*, our first radiative quantity. In physics this quantity is more frequently called spectral radiance. It is worth taking a moment to reflect on the subscript λ in I_λ. This quantity measures the fraction of the overall energy output per unit time that is radiated from the unit area dA in a certain direction, at a certain wavelength interval; thus, it is a *distribution* itself. It tells us how much energy the photons that hit our detector in a certain instant of time will carry with them. This energy can change at the very next instant of time, but we concern ourselves only with the energy carried during the time interval $[t,\ t+dt]$. This leaves the distribution of energy across wavelengths as the primary variable, hence the subscript λ. What we *really* mean, thus, is $I_\lambda \equiv dI/d\lambda$, i.e., a *distribution* of intensities per wavelength interval. If the radiator is a blackbody, this distribution would be prescribed by a Planck function B_λ:

$$B_\lambda = \frac{2hc^2}{\lambda^5}\frac{1}{\exp\left(\frac{hc}{\lambda kT}\right)-1}, \tag{4.2}$$

doi:10.1088/978-0-7503-1287-5ch4

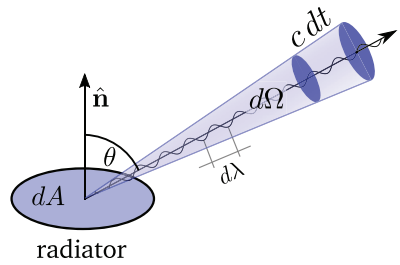

Figure 4.1. Definition of intensity: the amount of energy dE_λ per unit time dt per unit wavelength λ in a beam $d\Omega$ that is radiated from the direction-projected unit area $dA \cos\theta$.

where h is the Planck constant, c is the speed of light, k is the Boltzmann constant, and T is the effective temperature of the radiator. Thus, B_λ is the intensity that corresponds to a blackbody radiator with an effective temperature T. We could also use a sophisticated model that takes into account energy transfer through the outer layers of the star, shuffles photon numbers according to atomic transitions that cause spectral lines, and takes into account opacity variations along photon paths to predict intensity. Such models abound, and one of the well-established, freely accessible codes is that of Kurucz (2013). While the model atmosphere is substantially more complex compared to the Planck function, it still gives us the same quantity of interest: I_λ.

Before we move on, let us consider the units of intensity. It is easiest to do so by inspecting Equation (4.1) directly: we get J s^{-1} m^{-2} m^{-1} (do not let steradians fool you; they are not units), which yields watts per meter *cubed*. This is yet another reminder that we are implicitly referring to a distribution across λ.

4.2 Flux

It is time to introduce our second radiative quantity: flux. By definition, the flux through the radiative element dA is a net sum of all energy per unit time emitted through that element in all directions and projected along the normal of the unit area:

$$F_\lambda = \int_0^{2\pi} I_\lambda \cos\theta d\Omega \equiv \int_0^{\pi/2} \int_0^{2\pi} I_\lambda \cos\theta d\phi \sin\theta d\theta, \tag{4.3}$$

where ϕ and θ are longitudinal and latitudinal components of the solid angle with respect to the normal (i.e., $\theta = 0$ corresponds to the direction along the normal, and ϕ circumscribes the rings around the normal). In physics this quantity is more frequently called spectral flux density. To evaluate this integral, we need to ask ourselves whether I_λ depends on ϕ and/or θ. Strictly speaking, the intensity of real radiators likely does depend on both, but in an idealized case we may be able to get away with less stringent assumptions. In particular, it is reasonable to assume that the amount of energy irradiated along the same angle to the surface element normal is essentially the same, so I_λ will not depend strongly on ϕ. On the other hand, we *do* expect that intensity will depend on the angle to the surface element normal itself,

even if we do not know yet how exactly. So for the cylindrically isotropic case, Equation (4.3) can be simplified into:

$$F_\lambda = 2\pi \int_0^{\pi/2} I_\lambda(\theta)\cos\theta \sin\theta d\theta. \tag{4.4}$$

To figure out what drives the dependence of intensity on θ, consider layers upon layers in a stellar atmosphere, stacked like onion shells. Depending on the angle with respect to the surface element normal, the path traversed by a photon trying to escape will be different. The photon's best chance to escape will be along the normal, while any attempts perpendicular to the normal will be much more difficult. Hence, we expect more photons to be emitted along the normal than at an angle. It sounds like this dependence of I_λ on θ should depend on $\cos\theta$ since it is $\cos\theta$ that drives the length of the path taken by the photon through the outermost layer on its path to freedom, but let us be more general than that. First off, let us introduce $\mu = \cos\theta$ to save us from excessive writing, and then let us formulate a function $\mathcal{L}(\mu) = I_\lambda(\mu)/I_{\lambda,\,\mathrm{norm}}$, where $I_{\lambda,\,\mathrm{norm}}$ refers to the intensity along the normal, i.e., $\mu = 1$. If at this point you are tempted to nod and say "ah yes, the limb darkening function," hold that thought: we have not talked about any distribution of unit areas over the surface of the star; we limit our discussion only to the amount of light coming out of a *single* surface element dA. Equation (4.4) can now be rewritten as:

$$F_\lambda = 2\pi \int_1^0 I_\lambda(\mu)\mu(-d\mu) = 2\pi I_{\lambda,\,\mathrm{norm}} \int_0^1 \mu\mathcal{L}(\mu)d\mu. \tag{4.5}$$

Here we used a little algebraic trick $\sin\theta d\theta = -d(\cos\theta) \equiv -d\mu$ and took $I_{\lambda,\,\mathrm{norm}}$ in front of the integral since it does not depend on μ. The negative sign is absorbed by exchanging the integral boundaries. The flux can thus be thought of as normal emergent intensity scaled by $2\pi\int_0^1 \mu\mathcal{L}(\mu)d\mu$. Remember, though, that this has little to do with the flux that we detect as observers elsewhere; this is flux emanating from the unit area on the radiating body.

A closer look at Equation (4.5) can reveal a potential point of confusion: the units of flux appear to be the same as the units of intensity, namely, watts per meter cubed, whereas one might expect the units to be watts per meter *squared*. Do not let the established sloppiness in referring to flux density as "flux" confuse you: by F_λ we mean the *distribution* of flux across wavelengths, which is sometimes referred to as monochromatic flux. The actual flux is obtained by integrating over wavelength, and that will sort out the apparent units conundrum.

Now let us step away from the radiating body and place an observer at some arbitrary point at a distance D from the radiating unit area. The amount of energy radiated toward the observer is given by Equation (4.1):

$$dE_\lambda = I_\lambda(\theta)\, dt\, dA \cos\theta\, d\lambda\, d\Omega. \tag{4.6}$$

By the same equation, the amount of energy intercepted at the observer's point by a projected unit area dA' is:

$$dE'_\lambda = I'_\lambda(\theta')\, dt\, dA' \cos\theta'\, d\lambda\, d\Omega'. \tag{4.7}$$

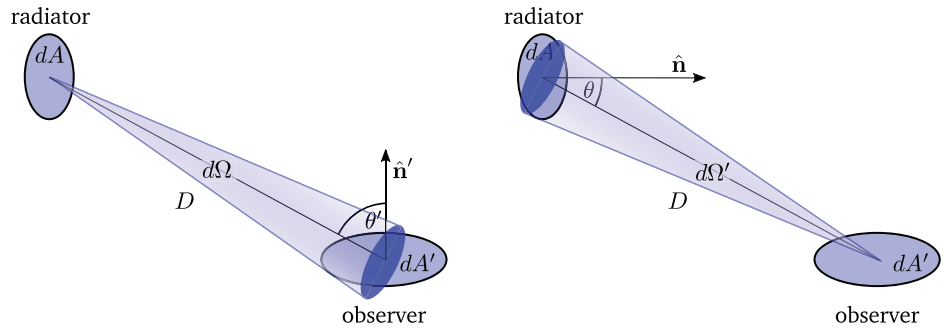

Figure 4.2. Different orientations of $d\Omega$ and $d\Omega'$ explain why $d\Omega$ is proportional to $A' \cos\theta'$ and $d\Omega'$ is proportional to $A \cos\theta$, i.e., Equation (4.8).

Note that $d\Omega$ and $d\Omega'$ are directed in the opposite sense: $d\Omega$ is a cone from the radiator to the observer, while $d\Omega'$ is a cone from the observer to the radiator (see Figure 4.2). If there is no attenuating matter between the emitting and intercepting unit areas, there is nothing to take away the energy, so it must be conserved: $dE_\lambda = dE'_\lambda$. At the same time, the solid angle differential $d\Omega$ depends on the distance and the projected intercepting area, while the solid angle differential $d\Omega'$ depends on the distance and the projected emitting area (as depicted in Figure 4.2):

$$d\Omega = \frac{dA'_\perp}{D^2} \equiv \frac{dA' \cos\theta'}{D^2}, \quad d\Omega' = \frac{dA_\perp}{D^2} \equiv \frac{dA \cos\theta}{D^2}. \tag{4.8}$$

Plugging these two expressions into Equations (4.6)–(4.7) immediately leads to two important conclusions: first, $I_\lambda(\theta) = I'_\lambda(\theta')$, i.e., the intensity of the beam is conserved and it does not depend on the distance, and second, $\mathcal{L}(\theta) = \mathcal{L}'(\theta')$, i.e., *now* it is appropriate to recognize that $\mathcal{L}(\theta)$ is indeed the limb-darkening function. This realization also allows us to compute the flux originating at the emitting unit area dA and flowing into the intercepting unit area dA' at the observer's location (see Figure 4.3):

$$dF_\lambda = I'_\lambda(\theta')\cos\theta' d\Omega' \equiv I_\lambda(\theta)\frac{\cos\theta' \cos\theta}{D^2} dA. \tag{4.9}$$

If the intercepting unit area is perpendicular to the beam (i.e., a detector pointing toward the light source), $\cos\theta' = 1$.

Suppose we now put a filter on the detector at the observer's location. This filter transmits only a part of the overall radiation and blocks the rest. Let its transmittance be described by a passband function $\mathcal{P}(\lambda)$. This reduces the amount of monochromatic flux on the detector to:

$$dF_\lambda = \mathcal{P}(\lambda) I_\lambda(\theta)\frac{\cos\theta' \cos\theta}{D^2} dA, \tag{4.10}$$

which we can interpret as $\mathcal{P}(\lambda)$ being a "sifting" function that determines how much of the intercepted flux on the $[\lambda, \lambda + d\lambda]$ interval actually reaches the detector. Any

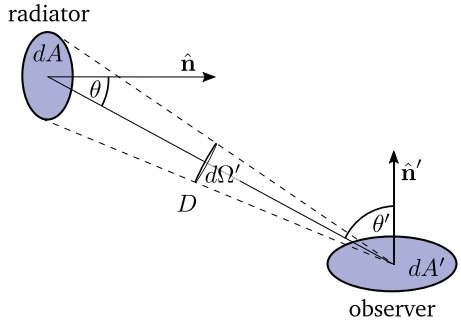

Figure 4.3. Amount of flux dF_λ intercepted at the observer's location.

real optics/detector system will cause further loss of radiation because of the inevitable efficiency limitations, and we can formally bundle all such effects into $\mathcal{P}(\lambda)$.

There is another consideration worth mentioning at this point: not all detectors are created equal in terms of what they measure. We are usually slack and say that the detector measures "light," but by that we mean either *energy*, which we have discussed so far, or *photon counts*. Depending on the quantity measured, detectors are either bolometric (measuring energy) or photoelectric (counting photons). Bolometric detectors have no notion of the number of photons detected, only their net energy; conversely, photoelectric detectors have no notion of energy, only the net number of photons. An example of a bolometric detector is a photoelectric photomultiplier. An example of a photoelectric detector is a charge coupled device (CCD). Because of this distinction, our equation for flux needs to be suitably adapted for the photon-counting instruments. The energy carried by a single photon on the wavelength interval $[\lambda, \lambda + d\lambda]$ is given by hc/λ, so the net energy at that wavelength interval is $dE_\lambda = dN_\lambda\, hc/\lambda$, where dN_λ is the number[1] of photons with wavelengths between λ and $\lambda + d\lambda$. Thus, if intensity is defined in terms of dN_λ instead of dE_λ, as appropriate for the photon-counting detectors, the expression for the passband flux becomes:

$$dF_\lambda^{\mathrm{pc}} = \frac{1}{hc}\,\lambda\mathcal{P}(\lambda)I_\lambda(\theta)\,\frac{\cos\theta'\cos\theta}{D^2}dA. \tag{4.11}$$

Here we used superscript "pc" to denote a photon-counting flux. Our realization from before that $\mathcal{L}(\theta) \equiv \mathcal{L}'(\theta')$ also allows us to express the monochromatic flux from the radiating unit area in the following form:

$$\begin{aligned} dF_\lambda &= \mathcal{P}(\lambda)I_{\lambda,\,\mathrm{norm}}\mathcal{L}(\mu)\frac{\mu\mu'}{D^2}dA, \\ dF_\lambda^{\mathrm{pc}} &= \frac{1}{hc}\,\lambda\mathcal{P}(\lambda)I_{\lambda,\,\mathrm{norm}}\mathcal{L}(\mu)\frac{\mu\mu'}{D^2}dA, \end{aligned} \tag{4.12}$$

[1] In our established practice of "slack" terminology, dN_λ is actually the *distribution* of the number photons per wavelength interval, indicated by the λ subscript.

where, as stated before, $\mu' \equiv \cos\theta' = 1$ in most[2] practical purposes.

Equations (4.12) set the stage for integration over the visible area of an extended body and over all wavelengths into the actual observed flux in absolute units (watts per meter squared). In the discussion that follows, we will derive expressions for bolometric detectors, but the results will be easily generalized to photon-counting devices as well.

In general, an extended body can have a complex shape, and parts of it may eclipse other parts; to describe this, let us introduce a visibility function $\mathcal{V}(\boldsymbol{r})$, where $\boldsymbol{r}$ gives the location on the radiating body surface, as:

$$\mathcal{V}(\boldsymbol{r}) = \begin{cases} 1 & \text{if } \mathrm{dA}(\boldsymbol{r}) \text{ is visible,} \\ 0 & \text{otherwise.} \end{cases} \tag{4.13}$$

The integral over the visible area can then still be performed over the entire surface ∂V of the radiating body with volume V,

$$F_\lambda = \frac{\mu'}{D^2}\mathcal{P}(\lambda)\int_{\partial V} \mu\mathcal{V}(\boldsymbol{r})I_{\lambda,\,\mathrm{norm}}\mathcal{L}(\mu)dA, \tag{4.14}$$

and the integral over all wavelengths (remember, $F_\lambda \equiv dF/d\lambda$) then yields the total flux:

$$F = \frac{\mu'}{D^2}\int_0^\infty \mathcal{P}(\lambda)\int_{\partial V} \mu\mathcal{V}(\boldsymbol{r})I_{\lambda,\,\mathrm{norm}}\mathcal{L}(\mu)dAd\lambda. \tag{4.15}$$

4.3 Luminosity

The final radiative quantity of interest to the current discussion is *luminosity*. By definition, luminosity is given by the net flux over all wavelengths over the radiating surface area:

$$L = \int_{\partial V}\int_{\lambda=0}^\infty F_\lambda d\lambda dA. \tag{4.16}$$

The units of luminosity are watts, implying that, indeed, luminosity is equivalent to what we would call *power* in physics. Note that luminosity is a property of the radiating body that is entirely independent of the position (or even the existence) of the observer: it measures the net energy output, and it will not change if it is near or far, or if something blocks it or reflects its light. It is an intrinsic property of the radiating body. Yet it still makes sense to ask what would be the luminosity of a radiating body in a given passband. It is crucially important not to think of this as a luminosity that somehow depends on the observational setup; instead, the question is how much power is in the spectral range defined by the $\mathcal{P}(\lambda)$ function. We call this passband luminosity and express it as:

$$L_{\mathrm{pb}} = \int_{\partial V}\int_0^\infty 2\pi\mathcal{P}(\lambda)I_{\lambda,\,\mathrm{norm}}\left(\int_0^1 \mu\mathcal{L}(\mu)d\mu\right)d\lambda dA. \tag{4.17}$$

[2] One notable exception is the treatment of reflection.

There are two important points to make here. First, bolometric luminosity can be considered a passband luminosity where the "passband" is simply $\mathcal{P}(\lambda) = 1$ for all λ. Thus, we can use $L_{\rm pb}$ for any luminosity, including bolometric, without any loss of generality. Second, it might seem surprising that luminosity depends on the limb-darkening function $\mathcal{L}(\mu)$; in this case, $\mathcal{L}(\mu)$ refers not to limb darkening but to the variation of intensity from the radiating unit area with direction μ; the equivalence with limb darkening stems from the conservation of intensity stemming from Equation (4.8). As we need to consider *all* radiated light, we certainly expect the dependence on $\mathcal{L}(\mu)$ or, more precisely, its integral over all μ.

4.4 Limb Darkening

So far we have made a few ad hoc references to the limb-darkening function $\mathcal{L}(\mu)$ without formally introducing the processes that shape its dependence on μ. As mentioned before, emergent intensity $I_\lambda(\mu)$ depends on the conditions in the stellar atmosphere. As light propagates outward, a fraction of it is absorbed by way of bound–bound transitions, bound–free absorption (photoionization), free–free absorption, and electron scattering. This extinction can be described by:

$$dI_\lambda = -\kappa_\lambda \rho I_\lambda dl, \tag{4.18}$$

where κ_λ is the absorption coefficient (or opacity), ρ is the local gas density, and dl is the path differential. The absorption coefficient κ_λ is generally a function of the wavelength, composition, density, and temperature of the gas: $\kappa_\lambda = \kappa_\lambda([\mathrm{M/H}], \rho, T_{\rm eff})$.

At the same time, some of the light is added to intensity by way of scattering, bound–bound emission, and recombination:

$$dI_\lambda = j_\lambda \rho dl, \tag{4.19}$$

where j_λ is the emission coefficient of the gas that generally depends on the same conditions as κ_λ. Note one important distinction, though: the contribution of emission to the emergent intensity is independent of the intensity I_λ itself. The reason is that this extra emission comes from the surrounding gas and thus has nothing to do with intensity itself.

The *net* change in emergent intensity is the sum of both emission and absorption:

$$dI_\lambda = j_\lambda \rho dl - \kappa_\lambda \rho I_\lambda dl. \tag{4.20}$$

The ratio of the rates at which the competing processes of emission and absorption occur determines how rapidly the intensity changes as it propagates layer after layer through the atmosphere. Dividing Equation (4.20) by $(-\kappa_\lambda \rho dl)$ yields:

$$-\frac{1}{\kappa_\lambda \rho}\frac{dI_\lambda}{dl} = I_\lambda - \frac{j_\lambda}{\kappa_\lambda} \equiv I_\lambda - \mathcal{S}_\lambda, \tag{4.21}$$

where $\mathcal{S}_\lambda = j_\lambda/\kappa_\lambda$ is called the source function and the equation in this form is called the *equation of radiative transfer*. The term $1/\kappa_\lambda \rho$ has a special significance: it

determines a typical attenuation length[3] and is called the *mean free path*. We can now define *optical depth* as $d\tau_\lambda = -\kappa_\lambda \rho dl$, where the negative sign implies that we measure it from the top of the stellar atmosphere inward. Based on the optical depth of the material, we can define its optical *thickness*: for $\tau_\lambda \gg 1$ the gas is said to be optically *thick*, while for $\tau_\lambda \ll 1$ it is said to be optically *thin*. Using optical depth, Equation (4.21) can be written as:

$$\frac{dI_\lambda}{d\tau_\lambda} = I_\lambda - \mathcal{S}_\lambda. \tag{4.22}$$

This is a nonhomogeneous differential equation of the first order. If the dependence of the source function $\mathcal{S}_\lambda$ on the optical depth τ_λ were known, Equation (4.22) could be solved to find emergent intensity as a function of μ. This is what model atmospheres do: they predict, using complex machinery, $\mathcal{S}_\lambda$ throughout the stellar photosphere. Simplified approximations for $\mathcal{S}_\lambda$ exist that allow analytical treatment, but at this point we will forgo the mathematical rigor in deriving the explicit relationship between the emergent intensity and an assumed modeling function for $\mathcal{S}_\lambda$ because it is lengthy and not really all that important for the discussion; instead, let us qualitatively review the main points of the process and refer those interested in full derivation to Gray (2008).

First, it is not immediately evident where μ enters Equation (4.22). Recall that $d\tau_\lambda = -\kappa_\lambda \rho dl$, i.e., the optical depth refers to opacity along the path dl, *whatever* the direction of dl may be. If we were to write dI_λ/dl in polar coordinates, for example, it would be:

$$\frac{dI_\lambda}{dl} = \frac{\partial I_\lambda}{\partial r}\frac{dr}{dl} + \frac{\partial I_\lambda}{\partial \theta}\frac{d\theta}{dl}. \tag{4.23}$$

In cases where the thickness of the visible atmosphere is small compared to the size of the radiator, we can neglect the second term on the right (i.e., we assume the plane-parallel approximation). At the same time, dr/dl is a projection of the path onto the radius vector, which is precisely μ—i.e., the dependence we were looking for —rendering the transfer equation to:

$$\mu\frac{dI_\lambda}{d\tau_{\lambda,\mu}} = I_\lambda - \mathcal{S}_\lambda, \tag{4.24}$$

where we denote with $\tau_{\lambda,\mu}$ the optical depth along the line of sight determined by μ.

Next, we need to ask ourselves how "deep" into the star we can see. The optical depth at the top of the atmosphere is 0, and it increases gradually toward the center of the star. The *photosphere* is a part of the overall stellar atmosphere from where the light we see originates; hence, it determines the effective temperature and the size of the star. This depth generally delimits the outer region of the star where

[3] This can be seen easily from the solution of Equation (4.18), $I_\lambda = I_{\lambda,0}\exp(-\kappa_\lambda \rho L)$.

photons scatter on average less than once on their way out. Even though formally we need to integrate τ_λ all the way to infinity, the exponentially growing optical depth ascertains rapid convergence of the integral in Equation (4.24). This is why the Sun does not appear "fuzzy"—the photosphere is quite thin compared to the star itself. Eddington has shown that, under the assumption of a gray atmosphere (i.e., κ_λ and j_λ do not depend on λ), the photosphere base is at an optical depth of 2/3. The actual depth will depend on the wavelength, of course—that is why we can "x-ray" the Sun. We generally consider that, in the optical, the photosphere is essentially opaque at $\tau_\lambda \sim 1$.

To compute emergent intensity in a given direction, we then need to integrate Equation (4.24) from the top of the photosphere to the depth at which opacity makes the interior opaque. This will be the same *optical* depth but a different *physical* depth depending on the angle to the surface normal we look at (see Figure 4.4). If we are looking at the center, the optical depth path is antiparallel to the radius and we will see the deepest, hottest, brightest layers. If we are looking toward the limb, the optical depth path is nearly perpendicular and we will see the shallowest, coolest, dimmest layers. In effect, we will see surface brightness variation because $\mathcal{S}_\lambda$ is different for each photosphere layer. It is this surface brightness variation that we see as limb darkening. We parameterize it by describing $I_\lambda(\mu)/I_{\lambda,\,\mathrm{norm}}$ as a function of μ. There are several models commonly used today; they are summarized in Table 4.1.

Note that the plane-parallel approximation embedded in Castelli & Kurucz (2004) model atmospheres breaks down for giant and supergiant stars. The effects of surface curvature are pronounced, and advanced treatment of atmospheres is necessary. There are several models that take curvature into account, for example, Phoenix/NextGen (Hauschildt et al. 1999) and SAtlas (Lester & Neilson 2008). NextGen models have been successfully integrated into the binary star modeling code ELC (Orosz & Hauschildt 2000). The curvature significantly affects the limb darkening, and the coefficients interpolated from the Castelli & Kurucz (2004) tables will likely be inadequate for giants and supergiants. Tables computed from spherical models, i.e., by Claret & Bloemen (2011), Neilson & Lester (2013), and similar works, should be considered instead.

4.5 Computational Efficiency

We now digress for a moment to address an important computational aspect of Equations (4.15) and (4.17). Recall that $\mathcal{P}(\lambda)I_{\lambda,\,\mathrm{norm}}(\lambda)$ corresponds to the passband-attenuated monochromatic intensity in the direction along the normal of the radiating unit area; if we integrate this expression over all wavelengths, we will get a normal emergent passband intensity:

$$I_{\mathrm{pb,\,norm}} = \int_0^\infty \mathcal{P}(\lambda)I_{\lambda,\,\mathrm{norm}}(\lambda)d\lambda \equiv \int_{\lambda_{\mathrm{lower}}}^{\lambda_{\mathrm{upper}}} \mathcal{P}(\lambda)I_{\lambda,\,\mathrm{norm}}(\lambda)d\lambda, \tag{4.25}$$

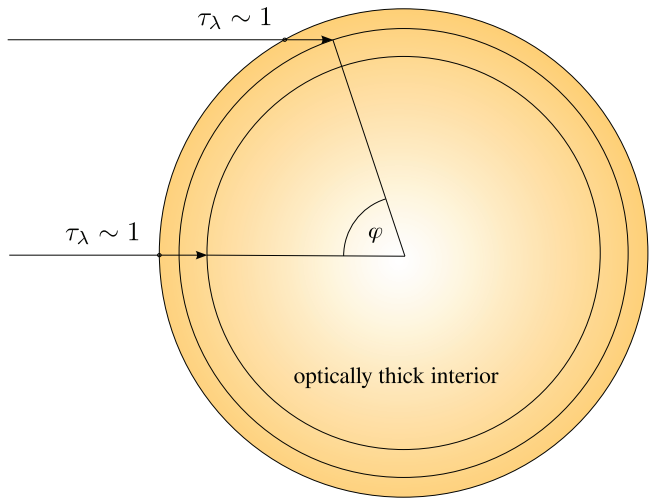

Figure 4.4. Limb-darkening effect. A common way to analytically quantify the optical depth of the visible photospheric surface is to adopt a model of a plane-parallel atmosphere. When the atmosphere is assumed to be gray (i.e., κ_λ is independent of λ), the reference surface by Eddington's approximation corresponds to the layer at optical depth $\tau_\lambda = 2/3$. This is a limited approximation because all sources of opacity except for Thompson scattering are wavelength dependent, but in general the reference layer will be at the optical depth of ~1.

Table 4.1. Table of Commonly Used Limb-darkening Models

Model	Functional Form	References
Linear	$\mathcal{L}(\mu) = 1 - x_\lambda(1-\mu)$	1
Logarithmic	$\mathcal{L}(\mu) = 1 - x_\lambda(1-\mu) - y_\lambda \mu \log(\mu)$	2
Square root	$\mathcal{L}(\mu) = 1 - x_\lambda(1-\mu) - y_\lambda(1-\sqrt{\mu})$	3
Quadratic	$\mathcal{L}(\mu) = 1 - x_\lambda(1-\mu) - y_\lambda(1-\mu)^2$	4
Exponential	$\mathcal{L}(\mu) = 1 - x_\lambda(1-\mu) - y_\lambda(1-\exp\mu)^{-1}$	5
Power	$\mathcal{L}(\mu) = 1 - a_{\lambda,1}(1-\mu^{1/2}) - a_{\lambda,2}(1-\mu) - a_{\lambda,3}(1-\mu^{3/2}) - a_{\lambda,4}(1-\mu^2)$	6
Interpolated	$\mathcal{L}(\mu) = \text{interp}\,(\mu;\, T_{\rm eff}, \log g, [\text{M/H}])$	7

References. (1) Schwarzschild 1906; (2) Klinglesmith & Sobieski 1970; (3) Diaz-Cordoves & Gimenez 1992; (4) Kopal 1950; (5) Claret & Hauschildt 2003; (6) Claret 2000; (7) Prša et al. 2016b.

where $\lambda_{\rm lower}$ and $\lambda_{\rm upper}$ are the limiting wavelengths of $\mathcal{P}(\lambda)$, i.e., the wavelengths below which and above which $\mathcal{P}(\lambda) = 0$, respectively. It proves computationally more practical to work with the *mean* normal passband intensity, computed as:

$$\langle I_{\rm pb,\,norm}\rangle = \frac{\int_\lambda \mathcal{P}(\lambda) I_{\lambda,\,\rm norm}(\lambda) d\lambda}{\int_\lambda P(\lambda) d\lambda} \equiv \frac{I_{\rm pb,\,norm}}{\int_\lambda P(\lambda) d\lambda}. \tag{4.26}$$

Plugging this into Equation (4.15) yields the passband flux,

$$F_{\rm pb} = \frac{\mu'}{D^2}\left(\int_\lambda \mathcal{P}(\lambda)d\lambda\right)\int_{\partial V}\langle I_{\rm pb,\,norm}\rangle\mu\mathcal{V}(\mathbf{r})\mathcal{L}(\mu)dA, \tag{4.27}$$

and an equivalent expression for the photon-counting devices,

$$F^{\rm pc}_{\rm pb} = \frac{\mu'}{D^2}\left(\frac{1}{hc}\int_\lambda \lambda\mathcal{P}(\lambda)d\lambda\right)\int_{\partial V}\langle I^{\rm pc}_{\rm pb,\,norm}\rangle\mu\mathcal{V}(\mathbf{r})\mathcal{L}(\mu)dA. \tag{4.28}$$

The reason why Equations (4.27)–(4.28) are more practical than Equation (4.15) is that the mean normal passband intensities $\langle I_{\rm pb,\,norm}\rangle$ and $\langle I^{\rm pc}_{\rm pb,\,norm}\rangle$ can be computed ahead of time from model atmospheres, and $\int_\lambda \mathcal{P}(\lambda)d\lambda$ and $(hc)^{-1}\int_\lambda \lambda\mathcal{P}(\lambda)d\lambda$ depend only on the transmission functions, so they can be computed in advance as well.

We can do the same for the luminosity computation:

$$L_{\rm pb} = \left(\int_0^\infty \mathcal{P}(\lambda)d\lambda\right)\int_{\partial V} 2\pi\langle I_{\rm pb,\,norm}\rangle\left(\int_0^1 \mu\mathcal{L}(\mu)d\mu\right)dA, \tag{4.29}$$

or, for the photon-counting detectors,

$$L^{\rm pc}_{\rm pb} = \left(\frac{1}{hc}\int_0^\infty \lambda\mathcal{P}(\lambda)d\lambda\right)\int_{\partial V} 2\pi\langle I^{\rm pc}_{\rm pb,\,norm}\rangle\left(\int_0^1 \mu\mathcal{L}(\mu)d\mu\right)dA. \tag{4.30}$$

In conclusion, the radiation in absolute units can thus be described by two pairs of equations, summarized in Table 4.2.

Turning to limb darkening, it is impractical to include the computation of limb-darkening coefficients in light-curve generators on the fly because of the complexity and numerical time cost of stellar atmosphere models. We instead resort to precomputed lookup tables. These are generated by synthesizing $I_\lambda(\mu)$ in absolute units from model atmospheres across the valid ranges of $T_{\rm eff}$, $\log g$, [M/H], and possibly other relevant atmospheric parameters and computing $I_\lambda(\mu)/I_{\lambda,\,\rm norm}$ for each set of parameters. We then fit any of the laws in Table 4.1 to these data to obtain the best-fit coefficients. Figure 4.5 depicts an example of a Sun-like limb darkening (filled circles), with fits for several limb-darkening models overplotted. It is clear that one- and even two-parameter models are not adequate for high-precision modeling.

Table 4.2. Equations That Govern the Computation of Flux from and Luminosity of a Radiating Body

Parameter	Equations
Passband flux	$F_{\rm pb} = \frac{\mu'}{D^2}(\int_\lambda \mathcal{P}(\lambda)d\lambda)\int_{\partial V}\langle I_{\rm pb,\,norm}\rangle\mu\mathcal{V}(\mathbf{r})\mathcal{L}(\mu)dA$
	$F^{\rm pc}_{\rm pb} = \frac{\mu'}{D^2}(\frac{1}{hc}\int_\lambda \lambda\mathcal{P}(\lambda)d\lambda)\int_{\partial V}\langle I^{\rm pc}_{\rm pb,\,norm}\rangle\mu\mathcal{V}(\mathbf{r})\mathcal{L}(\mu)dA$
Passband luminosity	$L_{\rm pb} = (\int_0^\infty \mathcal{P}(\lambda)d\lambda)\int_{\partial V} 2\pi\langle I_{\rm pb,\,norm}\rangle(\int_0^1 \mu\mathcal{L}(\mu)d\mu)dA$
	$L^{\rm pc}_{\rm pb} = (\frac{1}{hc}\int_0^\infty \lambda\mathcal{P}(\lambda)d\lambda)\int_{\partial V} 2\pi\langle I^{\rm pc}_{\rm pb,\,norm}\rangle(\int_0^1 \mu\mathcal{L}(\mu)d\mu)dA$

Note. Terms in angle brackets and in parentheses can be computed ahead of time to make the computation efficient.

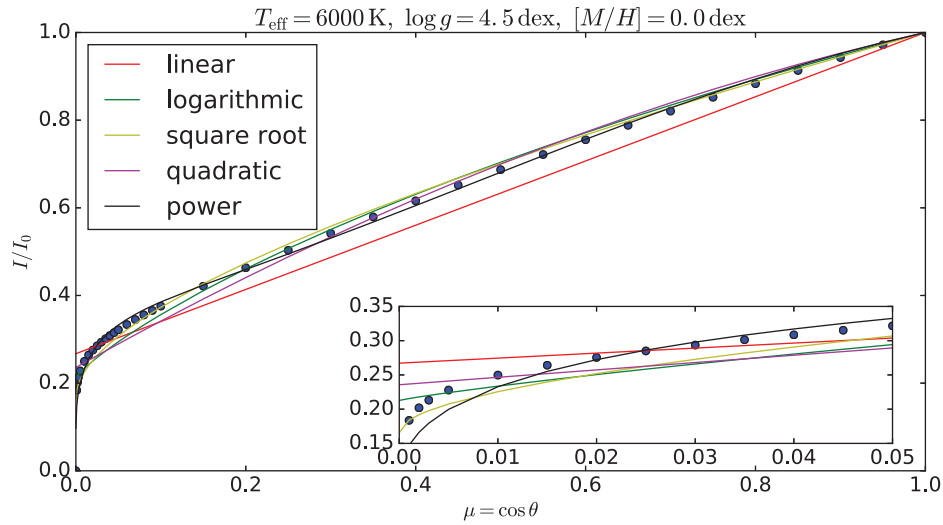

Figure 4.5. Variation of emergent passband intensity (with respect to normal emergent passband intensity) with emergent angle $\mu \equiv \cos\theta$. The inset shows a zoomed-in region at low μ. Filled circles are integrated intensities based on Castelli & Kurucz (2004) model atmospheres, and lines correspond to the fitted limb-darkening models using least squares. Systematics that arises from using these low-parametric models can be significant.

Further cuts in the parameter space spun by limb-darkening coefficients based on physical considerations can be made efficiently (Kipping 2013; Espinoza & Jordán 2016), but ultimately the accuracy of limb-darkening treatment will be limited either by the quality of the model fit or by the systematics in model atmospheres.

4.6 Relative Units

Our discussion so far has pertained to intensities, fluxes, and luminosities expressed in absolute physical units. However, in many use cases in astronomy this is not warranted or even possible, i.e., when we only have differential photometry, or we do not know the distance to the object, or we do not know the object's effective temperature accurately, or any combination of these and other limitations. The ongoing *Gaia* mission (Brown et al. 2016) holds the promise to change that by providing us with microarcsecond parallaxes, but until then, a common case calls for *relative* instead of absolute units.

What do the relative units entail? By relative we mean to say that whatever units are implied by the passband luminosity, those units are carried over to other radiative quantities. These can still be physical, of course, but more often they are referential, i.e., they yield a flux that allows direct comparison with observations that can be scaled[4] more or less arbitrarily. By *assigning* a certain passband luminosity,

[4] A common practice is to flux-normalize the data at some reference time stamp and use that as a point of reference that determines passband luminosity.

we are essentially imposing a scaling $\xi = L_{\mathrm{pb}}^{\mathrm{rel}}/L_{\mathrm{pb}}^{\mathrm{abs}}$ that satisfies the following relationship:

$$\begin{aligned} L_{\mathrm{pb}}^{\mathrm{rel}} &= \left(\int_0^\infty \mathcal{P}(\lambda)d\lambda\right)\int_{\partial V} 2\pi\langle I_{\mathrm{pb,\,norm}}^{\mathrm{rel}}\rangle\left(\int_0^1 \mu\mathcal{L}(\mu)d\mu\right)dA \\ \xi L_{\mathrm{pb}}^{\mathrm{abs}} &= \xi\left(\int_0^\infty \mathcal{P}(\lambda)d\lambda\right)\int_{\partial V} 2\pi\langle I_{\mathrm{pb,\,norm}}^{\mathrm{abs}}\rangle\left(\int_0^1 \mu\mathcal{L}(\mu)d\mu\right)dA, \end{aligned} \tag{4.31}$$

from which it follows directly that $\xi = \langle I_{\mathrm{pb,\,norm}}^{\mathrm{rel}}\rangle/\langle I_{\mathrm{pb,\,norm}}^{\mathrm{abs}}\rangle$. Thus, all equations in Table 4.2 retain their form; they are only multiplied by ξ to transform to the relative units suitably.

When we want to use photon counts to correctly weigh the data gathered by a photon-counting device but want to express the values in energy units, it helps to realize that:

$$L_{\mathrm{pb}} = F_{\mathrm{pb}}A, \quad L_{\mathrm{pb}}^{\mathrm{pc}} = F_{\mathrm{pb}}^{\mathrm{pc}}A \quad \Rightarrow \quad \frac{L_{\mathrm{pb}}^{\mathrm{pc}}}{L_{\mathrm{pb}}} = \frac{F_{\mathrm{pb}}^{\mathrm{pc}}}{F_{\mathrm{pb}}}. \tag{4.32}$$

This holds true for both absolute and relative units because the scaling factor ξ is canceled out. Thus, if ξ is the correct scaling factor for energy-weighted intensities, the same factor will scale the photon-weighted intensities as well.

4.7 Blackbody Radiation

The fundamental assumption of blackbody radiation is local thermodynamic equilibrium (LTE) of the radiator itself: whatever net energy flows into any part of the radiator, the same net energy leaves that part of the radiator, implying that the radiation within any unit volume of a blackbody radiator is *isotropic*. It is not just cylindrically isotropic, as was the case in Equation (4.4); it is *truly* isotropic, in all directions. For a blackbody radiator that means that whatever energy flows from the interior to the surface will be emitted to the exterior, none will be reflected back, and the amount of energy emitted will depend only on the effective temperature. Just *how* that energy will be radiated out is governed by the fact that the radiation inside is isotropic, implying that the radiation outward must also be isotropic. This has a fundamental implication: from whichever direction we look at a unit area of a blackbody radiator, we will see the same intensity. In other words, $I_\lambda(\mu)$ is equal to $I_{\lambda,\,\mathrm{norm}}$ for all μ, implying $\mathcal{L}(\mu) \equiv 1$:

$$F_\lambda = 2\pi I_{\lambda,\,\mathrm{norm}}\int_0^1 \mu d\mu = \pi I_{\lambda,\,\mathrm{norm}} \equiv \pi B_\lambda, \tag{4.33}$$

where $B(\lambda)$ is the Planck function given by Equation (4.2). This is known as Lambert's cosine law, where the "cosine" part refers to the term $\mu \equiv \cos\theta$ inside the integral. Integrating Equation (4.33) over all wavelengths then yields total flux:

$$F = \pi\int_0^\infty B_\lambda d\lambda = \pi\frac{\sigma}{\pi}T^4 \equiv \sigma T^4. \tag{4.34}$$

Here $\sigma = 2\pi^5 k^4/15h^3c^2$ is the Stefan–Boltzmann constant, and Equation (4.34) is known as Stefan's law.

The source function (Equation (4.22)) of a blackbody radiator is also of notable interest: it is equal to the Planck function B_λ, given by Equation (4.2). This is because pure emission and pure absorption of a blackbody are exactly balanced. As I_λ is constant, $dI_\lambda/dl = 0$ and $\mathcal{S}_\lambda = I_\lambda = B_\lambda$. This is important for stellar atmospheres, since the blackbody assumption of LTE immediately implies that the source function $S_\lambda = B_\lambda$.

To get blackbody flux in terms of photon counts instead, we do the same as before: we replace dE_λ with dN_λ in the expression for intensity, from which it immediately follows that $I_\lambda^{\text{pc}} = \lambda I_\lambda/hc$ and, from Equation (4.34),

$$F^{\text{pc}} = \frac{\pi}{hc}\int_0^\infty \lambda B_\lambda d\lambda = 4\pi c\left(\frac{k}{hc}\right)^3 \zeta(3)T^3, \tag{4.35}$$

where $\zeta(3) = 1.2020569\cdots$ is the Riemann zeta function. Combining Equations (4.34) and (4.35) allows us to express F^{pc} with F as:

$$\begin{aligned} F^{\text{pc}} &= 4\pi c\left(\frac{k}{hc}\right)^3 \frac{\zeta(3)}{\sigma^{3/4}} F^{3/4} \\ &= (4.137774 \times 10^{20}\text{s}^{-1}\text{m}^{-1/2}\text{W}^{-3/4})F^{3/4}. \end{aligned} \tag{4.36}$$

Analogously, the relationship between the luminosity in photon counts per second and luminosity in watts can be derived by observing that $L^{\text{pc}}/L = F^{\text{pc}}/F$, from which it immediately follows that:

$$L^{\text{pc}} = 4\pi c\left(\frac{k}{hc}\right)^3 \frac{\zeta(3)}{\sigma^{3/4}} A^{1/4} L^{3/4}, \tag{4.37}$$

where A is the surface area of the radiating body.

There is another subtlety with blackbody radiators that we need to take into account: we need to ensure consistency across luminosity and flux in the presence of limb darkening. This is tricky because, according to Lambert's law (Equation (4.33)), a blackbody disk would appear uniformly bright, i.e., there would be no inherent limb darkening. Stars, of course, are limb darkened, so any $\mathcal{L}(\mu) \neq 1$ applied to blackbody fluxes will cause the luminosity to change. This is a problem because $I_{\lambda,\,\text{norm}}$ depends solely on the temperature (Equation (4.2)), and when integrated over the surface area of a star, it yields luminosity (Equation (4.16)) that is independent of any limb darkening:

$$L = \int_{\partial V}\int_0^\infty F_\lambda d\lambda dA = \int_{\partial V} \sigma T^4 dA = \sigma T^4 A. \tag{4.38}$$

When we apply the limb-darkening correction, we reduce the flux that corresponds to the effective temperature, thus causing a discrepancy between the actual effective temperature and the "apparent" effective temperature. Say, for example, that $\mathcal{L}(\mu) = 0.5$ for all μ: that would reduce F_λ by a factor of 2 across the board, implying

that the "apparent" effective temperature is a factor of $2^{1/4}$ smaller than the actual effective temperature—hence the discrepancy. To ensure consistency between luminosity and flux, it is $I_{\lambda,\,\mathrm{norm}}$ in Equation (4.5) that needs to increase by the amount that limb darkening decreases the flux. In other words, Equation (4.5) for blackbody radiators becomes:

$$F_{\lambda,\,\mathrm{bb}} = 2\pi\left(\frac{I_{\lambda,\,\mathrm{norm}}}{\int_0^1 \mu\mathcal{L}(\mu)d\mu}\right)\int_0^1 \mu\mathcal{L}(\mu)d\mu, \tag{4.39}$$

where the quantity in parentheses is our effective monochromatic blackbody intensity, which is larger than the Planckian intensity by the overall amount reduced by limb darkening. When integrated over the surface, this will yield the luminosity that corresponds to the actual effective temperature, not to the "apparent" effective temperature.

4.8 Putting It All Together

Equipped with the framework developed so far, we can now dive into our example: the Sun–Earth system within the blackbody approximation and with model atmospheres. The reader is strongly encouraged to take this opportunity and work through the examples with a calculator in hand.

We start by assigning the following numerical values to the Sun (Prša et al. 2016a):

Luminosity:	$L_\odot = 1\ \mathcal{L}_\odot^{\mathrm{N}} \equiv 3.828 \times 10^{26}$ W
Radius:	$R_\odot = 1\ \mathcal{R}_\odot^{\mathrm{N}} \equiv 6.957 \times 10^{8}$ m
Effective temperature:	$T_\odot = 1\ \mathcal{T}_\odot^{\mathrm{N}} \equiv 5.772 \times 10^{3}$ K
Synchronicity parameter:	$F_\odot = 14.61$

and the following numerical values to the orbit:

Mass ratio:	$q = \mathcal{GM}_{\mathrm{E}}^{\mathrm{N}}/\mathcal{GM}_\odot^{\mathrm{N}} = 3.003489 \times 10^{-6}$
Semimajor axis:	$a = 149,\ 597,\ 870,\ 700$m

Let us first compute analytical reference values for a spherical Sun that we will use as gauges for the numerical computation. The bolometric flux at Earth is:

$$F_{\mathrm{bol}} = \frac{\mathcal{L}_\odot^{\mathrm{N}}}{4\pi a^2} = \frac{3.828 \times 10^{26}\ \mathrm{W}}{4\pi(149,\ 597,\ 870,\ 700\ \mathrm{m})^2} = 1361.166\ \mathrm{Wm}^{-2}. \tag{4.40}$$

Using Equations (4.36) and (4.37), we can readily obtain bolometric radiative quantities in photon counts:

$$\begin{aligned} F_{\text{bol}}^{\text{pc}} &= 6.323 \times 10^{21} \text{ photons m}^{-2}\text{ s}^{-1}, \\ L_{\text{bol}}^{\text{pc}} &= 1.778 \times 10^{45} \text{ photons s}^{-1}. \end{aligned} \tag{4.41}$$

Now let us investigate how close we can get to the bolometric values by using a quasi-bolometric box passband:

$$\mathcal{P}(\lambda) = \begin{cases} 1 & \text{for } 90 \text{ nm} \leqslant \lambda \leqslant 4\,\mu\text{m} \\ 0 & \text{otherwise.} \end{cases} \tag{4.42}$$

This wavelength region is chosen because the list of spectral lines is most complete in this region, which will allow us to make a one-to-one comparison with model atmospheres later on. Thanks to our spherical Sun approximation, the equations in Table 4.2 are significantly simplified:

$$\begin{aligned} F_{\text{pb}} &= \Delta\lambda \langle I_{\text{pb, norm}} \rangle \pi \mathcal{R}_{\odot}^{\text{N}^2} / D^2 = 1347.879 \text{ Wm}^{-2}, \\ L_{\text{pb}} &= \Delta\lambda \pi \langle I_{\text{pb, norm}} \rangle 4\pi \mathcal{R}_{\odot}^{\text{N}^2} = 3.791 \times 10^{26} \text{ W}. \end{aligned} \tag{4.43}$$

Here we used $\langle I_{\text{pb, norm}} \rangle = \int_{90\text{ nm}}^{4\,\mu\text{m}} B_\lambda d\lambda / \Delta\lambda = 5.074 \times 10^{12}$ W m^{-3}. The percent difference between this quasi-bolometric passband and true bolometric values is ~1%.

Now let us do the same for the photon-counting devices. The equations in Table 4.2 simplify to:

$$\begin{aligned} F_{\text{pb}}^{\text{pc}} &= \mathcal{P}_{\text{int}}^{\text{pc}} \langle I_{\text{pb, norm}}^{\text{pc}} \rangle \pi \mathcal{R}_{\odot}^{\text{N}^2} / D^2 = 5.911 \times 10^{21} \text{ photons s}^{-1}\text{ m}^{-2}, \\ L_{\text{pb}}^{\text{pc}} &= \mathcal{P}_{\text{int}}^{\text{pc}} \pi \langle I_{\text{pb, norm}}^{\text{pc}} \rangle 4\pi \mathcal{R}_{\odot}^{\text{N}^2} = 1.662 \times 10^{45} \text{ photons s}^{-1}, \end{aligned} \tag{4.44}$$

where $\mathcal{P}_{\text{int}}^{\text{pc}} = \int_{\lambda} \lambda \mathcal{P}(\lambda) d\lambda / hc = 4.025 \times 10^{13}$ m J^{-1} and $\langle I_{\text{pb, norm}}^{\text{pc}} \rangle = 2.161 \times 10^{12}$ photons s^{-1} m^{-3}. The percent difference now is a whopping 7%. This is not surprising, though: the larger discrepancy comes from weighting the intensity integral by λ, so any photons redward of the 4 μm cutoff are additionally weighted. In other words, the flux in energy units diminishes as λ^4 at long wavelengths (the so-called Rayleigh–Jeans regime), but only as λ^3 in photon counts. If we extended the red cutoff to 8 μm, the percent difference in photon counts would dip below 1%.

Now let us "turn on" limb darkening. We will model $I(\mu)$ with a logarithmic limb-darkening law (see Table 4.1):

$$\frac{I(\mu)}{I_0} = 1 - x_\lambda(1 - \mu) - y_\lambda\, \mu \ln \mu, \tag{4.45}$$

where x_λ and y_λ are passband-dependent limb-darkening coefficients. Their values depend on atmospheric parameters (effective temperature, surface gravity, heavy metal abundance, etc). For the Sun, the values are:

$$x_\lambda = 0.6923 \quad \text{and} \quad y_\lambda = 0.1628. \tag{4.46}$$

These were obtained by fitting $\mathcal{L}(\mu)$ to $I_\lambda(\mu)/I_{\lambda,\,\mathrm{norm}}$ values derived from Castelli & Kurucz (2004) model atmospheres within PHOEBE. For illustration purposes, let us use Equation (4.39) without correcting the Planckian intensity to demonstrate why this is a problem.

With limb darkening in effect, the $\mathcal{L}(\mu)$ integral is no longer unity; logarithmic $\mathcal{L}(\mu)$ is easily integrable:

$$\int_0^1 \mu\mathcal{L}(\mu)d\mu = \int_0^1 \mu[1 - x_\lambda(1-\mu) - y_\lambda\mu\ln\mu] = 1 - \frac{1}{3}x_\lambda + \frac{2}{9}y_\lambda. \tag{4.47}$$

For the values given in Equation (4.46), this expression evaluates to $\mathcal{L}_{\mathrm{int}} = 0.8054$. Using energy-weighted equations in Table 4.2 yields:

$$\begin{aligned} L_{\mathrm{pb}} &= \Delta\lambda \int_0^{4\pi R^2} 2\pi\langle I_{\mathrm{pb,\,norm}}\rangle\mathcal{L}_{\mathrm{int}}dA = 3.053\times 10^{26}\ \mathrm{W}, \\ F_{\mathrm{pb}} &= \frac{\Delta\lambda}{D^2}\int_0^{2\pi R^2} \langle I_{\mathrm{pb,\,norm}}\rangle\mu\mathcal{L}(\mu)dA = 1085.323\ \mathrm{Wm^{-2}}. \end{aligned} \tag{4.48}$$

These values should raise a red flag: the intensities $\langle I_{\mathrm{pb,\,norm}}\rangle$ and limb-darkening coefficients were computed for $T_{\mathrm{eff}} = 5772$ K, but the flux we obtain corresponds to 5468 K. The difference corresponds precisely to $\mathcal{L}_{\mathrm{int}}$ (its 1/4 power, to be exact) in Equation (4.39). Thus, if we replace $I_{\lambda,\,\mathrm{norm}}$ with $I_{\lambda,\,\mathrm{norm}}/\mathcal{L}_{\mathrm{int}}$, we reproduce the expected values:

$$\begin{aligned} L_{\mathrm{pb}} &= \Delta\lambda \int_0^{4\pi R^2} 2\pi\langle I_{\mathrm{pb,\,norm}}\rangle dA = 3.791\times 10^{26}\ \mathrm{W}, \\ F_{\mathrm{pb}} &= \frac{\Delta\lambda}{D^2}\int_0^{2\pi R^2} \frac{\langle I_{\mathrm{pb,\,norm}}\rangle}{\mathcal{L}_{\mathrm{int}}}\mu\mathcal{L}(\mu)dA = 1347.539\ \mathrm{Wm^{-2}}. \end{aligned} \tag{4.49}$$

The same procedure applies to the photon-weighted values, yielding:

$$\begin{aligned} F_{\mathrm{pb}}^{\mathrm{pc}} &= 5.909\times 10^{21}\ \text{photons s}^{-1}\,\mathrm{m}^{-2}, \\ L_{\mathrm{pb}}^{\mathrm{pc}} &= 1.662\times 10^{45}\ \text{photons s}^{-1}. \end{aligned} \tag{4.50}$$

Switching now to model atmospheres, there is one important caveat to be aware of: I_μ already "contains" the information about limb darkening by way of the numerically estimated source function $\mathcal{S}_\lambda$. Thus, if limb darkening is turned off, we *expect* that both the luminosity and flux are overestimated. This does not technically make the solution inconsistent: if there were no limb darkening, those would be true luminosity and flux values; the culprit for an apparently inconsistent result is the unphysical assumption that we make by switching off limb darkening.

Beyond that consideration, all other principles used in blackbody computation remain the same. That is why we summarize the numerical values in Table 4.3 and end the discussion by stressing yet again that, although relatively straightforward, the computation of radiative properties is wrought with intricacies that are further

Table 4.3. Luminosities, Fluxes, and Scaled Fluxes in Energy- and Photon-weighted Mode

LD Model	$L_{\rm pb}$ (W)	$F_{\rm pb}$ (W m^{-2})	$\xi F_{\rm pb}$ (W m^{-2})	$L_{\rm pb}^{\rm pc}$ (photons s^{-1})	$F_{\rm pb}^{\rm pc}$ (photons s^{-1} m^{-2})	$\xi F_{\rm pb}^{\rm pc}$ (W m^{-2})
None	4.714×10^{26}	1676.190	1347.909	2.031×10^{45}	7.224×10^{21}	1347.910
Logarithmic	3.797×10^{26}	1349.649	1347.538	1.636×10^{45}	5.816×10^{21}	1347.538
Interpolated	3.842×10^{26}	1365.777	1347.507	1.734×10^{45}	6.165×10^{21}	1347.560

Note. The values pertain to Castelli & Kurucz (2004) model atmospheres and solar atmospheric parameters.

complicated by the presence of another body in a system—a topic of the following section.

References

Brown, A. G. A., Vallenari, A., Prusti, T., et al. 2016, A&A, 595, A2
Castelli, F., & Kurucz, R. L. 2004, arXiv:astro-ph/0405087
Claret, A. 2000, A&A, 363, 1081
Claret, A., & Bloemen, S. 2011, A&A, 529, A75
Claret, A., & Hauschildt, P. H. 2003, A&A, 412, 241
Diaz-Cordoves, J., & Gimenez, A. 1992, A&A, 259, 227
Espinoza, N., & Jordán, A. 2016, MNRAS, 457, 3573
Gray, D. F. 2008, The Observation and Analysis of Stellar Photospheres (Cambridge: Cambridge Univ. Press)
Hauschildt, P. H., Allard, F., & Baron, E. 1999, ApJ, 512, 377
Kipping, D. M. 2013, MNRAS, 435, 2152
Klinglesmith, D. A., & Sobieski, S. 1970, AJ, 75, 175
Kopal, Z. 1950, HarCi, 454, 1
Kurucz, R. L. 2013, ATLAS12: Opacity Sampling Model Atmosphere Program, Astrophysics Source Code Library, ascl:1303.024
Lester, J. B., & Neilson, H. R. 2008, A&A, 491, 633
Neilson, H. R., & Lester, J. B. 2013, A&A, 556, A86
Orosz, J. A., & Hauschildt, P. H. 2000, A&A, 364, 265
Prša, A., Conroy, K. E., Horvat, M., et al. 2016a, ApJS, 227, 29
Prša, A., Harmanec, P., Torres, G., et al. 2016b, AJ, 152, 41
Schwarzschild, K. 1906, NWGot, 195, 41